Antibody recognition of chiral surfaces. Enantiomorphous crystals of leucine-leucine-tyrosine

ARTICLE *in* JOURNAL OF THE AMERICAN CHEMICAL SOCIETY · FEBRUARY 2003

Impact Factor: 12.11 · DOI: 10.1021/ja027942j · Source: PubMed

4 AUTHORS, INCLUDING:

Felix Frolow
Tel Aviv University
207 PUBLICATIONS **9,578** CITATIONS
SEE PROFILE

Miriam Eisenstein
Weizmann Institute of Science
164 PUBLICATIONS **5,872** CITATIONS
SEE PROFILE

Lia Addadi
Weizmann Institute of Science
252 PUBLICATIONS **18,043** CITATIONS
SEE PROFILE

Antibody Recognition of Chiral Surfaces. Structural Models of Antibody Complexes with Leucine–Leucine–Tyrosine Crystal Surfaces

Merav Geva,[1] Miriam Eisenstein,[2] and Lia Addadi[1]*
[1]*Department of Structural Biology, Weizmann Institute of Science, 76100 Rehovot, Israel*
[2]*Department of Chemical Services, Weizmann Institute of Science, Rehovot, Israel*

ABSTRACT **Molecular models are built of the recognition domains of two antibodies, which are raised and selected against crystals of (L)leucine-(L)leucine-(L)tyrosine. The model of one antibody, which is stereo- and enantioselective, reveals astounding chemical and structural complementarity to the recognized crystal surface. The enantioselective binding of this antibody is explained by the significantly fewer chemical interactions arising in the complex, after docking of the antibody to the (D)Leu-(D)Leu-(D)Tyr crystal face, relative to its enantiomer, the (L)Leu-(L)Leu-(L)Tyr crystal face. The modeling and docking of the second antibody, which is poorly stereoselective and is not enantioselective, indicates that binding is based on electrostatic interactions. The docking models of the antibody–crystal complexes provide a rationale for the experimental results while demonstrating the power of modeling techniques to meet the challenge of describing antibody–antigen interactions in detail. Proteins 2004; 55:862–873.** © **2004 Wiley-Liss, Inc.**

Key words: antibody–antigen complex; chiral discrimination; docking; enantioselectivity; molecular recognition; stereoselectivity; structural complementarity

INTRODUCTION

Antibodies are the tools that nature evolved in vertebrates to tag foreign invaders, such that they may be subsequently dealt with by the immune system. Tagging is achieved through molecular recognition. Antibodies bind their targets, the antigens, through interactions involving several loops that form the antigen binding site. These sites in different antibodies are structurally diverse, ranging from large flat surfaces to highly structured surfaces presenting complex features such as ridges and cavities.[1–3] Antibody–antigen interactions range from cross-reactivity to exquisite specificity, which is demonstrated by the ability to detect minute molecular differences between different antigens. Such high differentiation ability results from structural and chemical complementarity over a large surface area, which allows the establishment of favorable chemical interactions while avoiding steric repulsion at the interface.[4] Conversely, polyreactive or cross-reactive antibodies bind different antigens with similar affinity. The mechanism underlying cross-reactivity is unclear. One possibility is that some conformational flexibility of the binding site allows the antibody to bind several antigens.[4–9] Another option is that polyreactive antibodies expose in their binding sites an array of interactive moieties, including charge, which account for the possibility of various ligands being accommodated in the combining site.[4,8,10]

Crystal surfaces of various organic molecules were previously shown to be antigenic. Such peculiar antigens are characterized by a known repetitive structure, and they are not prone to undergo conformational changes. Monoclonal antibodies elicited against crystals of cholesterol monohydrate and dinitrobenzene were studied in some depth.[11–17] These antibodies show a wide variety of recognition patterns, ranging from preferential binding to one specific crystal face to preferential binding to various faces of one crystal, to nonspecific interactions with many surfaces of different crystals. One antibody, raised against cholesterol monohydrate crystals,[11] is highly stereoselective, insofar as it keenly distinguishes between monolayers of cholesterol and its epimer, epicholesterol.[15] It does not, however, show enantioselectivity, because it binds to the same extent to monolayers of cholesterol and of its enantiomer, ent-cholesterol.[16] The lack of enantioselectivity was attributed to the low level of chiral information expressed at the enantiomeric antigen surfaces. In other words, although the surfaces are chiral by definition, their chirality is not manifested at a level that is detectable by the antibody.[17]

In order to investigate the subtlest chiral recognition limit of antibodies for surfaces, we have recently used crystals of the tripeptide (L)leucine-(L)leucine-(L)tyrosine and its enantiomer (D)Leu-(D)Leu-(D)Tyr. These peptide crystals introduce antigenic surfaces that may resemble protein surfaces, to some extent. Furthermore, they explicitly introduce the challenge of chirality: enantiomeric peptides form enantiomeric crystals, which present a variety of surfaces that have the same physical and

Grant sponsor: Israel Science Foundation.

*Correspondence to: L. Addadi. E-mail: lia.addadi@weizmann.ac.il.

Received 13 July 2003; Revised 22 October 2003; Accepted 27 October 2003

Published online 6 April 2004 in Wiley InterScience (www.interscience.wiley.com). DOI: 10.1002/prot.20042

chemical characteristics but are mirror images of each other.

Monoclonal antibodies against crystals of (L)Leu-(L)Leu-(L)Tyr were produced by immunization of mice and selection of antibodies specific to the crystals. Notably, the selection occurs in the presence of soluble peptide molecules, forcing selection of antibodies that bind only to the crystals and not to the soluble peptide. Two antibodies were extensively studied.[18] One antibody is stereoselective and enantioselective, the other has limited stereoselectivity and no enantioselectivity. The stereoselectivity was manifested in selective antibody binding to one crystal face, relative to other faces of the same crystal having the same composition but different structural arrangements. The enantioselectivity was manifested in selective antibody binding to crystals of (L)Leu-(L)Leu-(L)Tyr and lack of binding to crystals of the enantiomorph (D)Leu-(D)Leu-(D)Tyr.

The wide spectrum of recognition selectivities of antibody–crystal interactions raises the inevitable question about the structural and chemical basis that is at the origin of such interactions. On the one hand, the fact that the antigen is a crystal surface prevents structural studies of the antibody–crystal complexes by X-ray crystallography, because the complex cannot be crystallized as such. On the other hand, it provides knowledge of the surface presented by the antigen at high resolution. Solving the structure of the antibody separately may provide information about the binding site. However, the structure of the unbound antibody may be different from its structure in the complex. Antigen binding is known to induce some conformational changes in the antibody binding site. This is expected to be particularly relevant for antibodies specific to crystals, whose binding site is a more or less open, extended surface.[19–23] As a viable alternative to obtain structural information on the antibody–antigen complexes, we apply modeling techniques.

Knowledge-based procedures for antibody structure modeling have been developed based on the highly conserved framework structure of antibodies[24] and the small repertoire of main-chain conformations for five of the six hypervariable complementarity-determining regions (CDRs)[25] and for the stem of the sixth CDR.[26] These procedures are based on amino acid sequence comparisons to known crystallographic structures. Thus, the quality of the model depends on the extent of similarity between the sequences, with emphasis on the CDRs and the heavy and light chain interface. (For a review, see Ref. 26.)

Comparative modeling was previously used to obtain structures of the binding domains of antibodies raised against crystals of cholesterol and dinitrobenzene.[27] The variable regions of the antibodies were sequenced, and the structures of their recognition sites were modeled. The models showed a remarkable structural and chemical complementarity between the antibody binding sites and the crystal surfaces they bind.

The impressive stereoselectivity and enantioselectivity experimentally exhibited by one antibody against the tripeptide leucine–leucine–tyrosine, and the low selectivity exhibited by the other, provide a valuable test case of the parameters active in antibody–antigen recognition, as well as the strength of the modeling techniques. The chemical and structural basis for the recognition of the two antibodies is studied in this work by modeling of the recognition sites of antibodies 48E and 602E, as well as their complexes with the relevant crystal surfaces.

MATERIALS AND METHODS

Materials and Equipment

TriReagent kit T9424 for total RNA extraction was purchased from Sigma Aldrich Israel ltd. (Rehovot, Israel). Reverse transcription was performed with an A3500 kit purchased from Promega Corp. (Madison, WI). Enzymes and buffers for polymerase chain reaction (PCR; BIO-X-ACT™ DNA polymerase M11801B kit) were purchased from Bioline Ltd. (London). The DNA isolation kit (20-200-300) for DNA extraction from agarose gel was purchased from Biological Industries Ltd. (Beit-HaEmek, Israel).

Computer-aided comparative modeling and structure analysis was done using the InsightII program (Accelrys Inc., San Diego, CA) on a Silicon Graphics workstation.

Antibody Cloning and Sequencing

Hybridoma cells were obtained from the monoclonal antibody unit (Biological Services), and total RNA was purified from the cells using TriReagent (Sigma) according to the manufacturer's instructions. cDNA was obtained by reverse transcription of the total RNA using an RT kit (Promega) according to the manufacturer's protocol. The heavy and light chain variable domain genes were amplified by the PCR. Amplification was performed with BIO-X-ACT DNA polymerase (Bioline) in an automated thermal cycler using cycles of 2-min incubation at 95°C; 25 cycles of 1-min incubation at 95°C; 1-min incubation at 40°C, and 2-min incubation at 72°C; and 4-min incubation at 72°C.

The following consensus oligonucleotide primers were used, according to Orlandi et al.[28]:

5′ terminus:

V_κ 5′-CCC AAG CTT GAC ATT GTG GTG ACC CAG TCT CCA (#3450)

V_H 5′-GCG AAT TCG TCG ACS AGG TSM ARC TGC AGS AGT CWG G (#5686)

3′ terminus:

J_κ 5′-CCC GAA TTC TTA GAT CTC CAG CTT GGT CCC (#3451)

C_κ 5′-GCG CCG TCT AGA TTA ACA CTC ATT CCT GTT GAA (#5174)

J_H 5′-TGA RGA GAC GGT GAC CAG GGT BCC (#1830)

C_{IgM} 5′-GCA CTA GTG CAC ATG TGG AGG ACA CG (#13532)

where S = G or C; M = A or C; R = A or G; W = A or T; and B = G, C, or T.

The PCR fragments were extracted from agarose gels by a DNA isolation kit (Biological Industries) and sequenced at the DNA sequencing unit (Biological Services, Weizmann Institute of Science) using the same primers that

were used for the PCR. The genes were sequenced on an automated sequencer at the DNA sequencing unit (Biological Services, Weizmann Institute of Science).

Antibody Modeling and Docking to Crystal Surfaces

Templates for modeling the light and heavy chains of each antibody were selected based on a comparison (FASTA[29,30]) of each sequence with the RCSB Protein Data Bank (PDB).[31] First, structures with the most similar sequences of the light or heavy chain Fv fragment were superimposed. Second, the relative positions of the heavy and light chain frameworks were examined. Preference was given to templates that could be used to model both light and heavy chains. Third, we preferred templates in which the L1, L2, L3, H1, and H2 loops have the same canonical structures as in the modeled antibody.

The initial models for the variable regions were generated using the Homology module of InsightII (Accelrys Inc., San Diego, CA), which is based on the crystallographic structure of the chosen templates. Energy minimization was performed using the Discover module with the consistent valence force field. The Cα atoms of the heavy and light chains, except for the H3 loop, were constrained to their initial positions.

Docking of the antibody models onto the different crystal faces was done using the geometric rigid body docking program MolFit.[32,33] The algorithm involves matching of the molecular surfaces by defining a surface layer for each molecule and distinguishing it from the interior. In this study, the crystal was fixed in space and one of its faces was defined as the "molecular surface." The antibody molecule was rotated to different orientations relative to the crystal and translated along three orthogonal axes. The quality of the surface geometric match was evaluated for each relative position, producing a complementarity score. This score is higher as the geometric complementarity is more extensive and there are no interpenetrations.[32,33] Because of the uncertainty in the modeling of the H3 loop of antibody 48E, its five apex residues were omitted during the docking search. MolFit was previously tested in blind prediction experiments in which a high success rate was attained.[34,35]

The MolFit rotation-translation scan was performed with a translational step of 1.1 Å and an angular interval of 10°. However, some orientations were not considered. The molecules were first oriented such that the pseudo twofold axis of the antibody was approximately parallel to the normal of the given crystal face and the CDRs faced the crystal surface. Only orientations in which the antibody deviated by less than 45° from the original geometry were considered. This limitation reflects the fact that the docking is done only with the variable region, not the whole IgM molecule. One solution with the highest complementarity score was saved for each orientation. All of the solutions were then sorted by their scores. The top ranking solutions were refined by recalculating the score for small angular deviations (±2°) about three perpendicular axes. A statistical analysis of the solutions in a given docking scan was done by fitting an extreme value distribution function[36] to the observed distribution of scores. This provided estimates for the mean score and the standard deviation (σ) in the given scan. For each crystal face the solutions with scores within the top 4σ were manually analyzed, yielding a few putative docking models. The apex of the H3 loop of antibody 48E, which was omitted in the docking scans, was added to each of the putative complexes using the "loop generation" option in the Homology module of InsightII.

The putative complexes were optimized using the Discover module of the InsightII package. Initially, all the C, N, O, and S atoms were fixed except in the H3 apex residues. Next, only the Cα was atoms were fixed, except in the H3 apex residues, so that free movement was allowed for the H3 apex and for all side chains. Finally, 5000 steps of dynamics (1-fs steps at 300 K) were performed, followed by energy minimization requiring convergence of the force derivative to 0.001. Note that all the atoms of the crystal, including hydrogens, were fixed throughout the optimization procedure.

RESULTS

Antibodies 48E and 602E, which showed drastically different reactivity toward the surfaces of (L)Leu-(L)Leu-(L)Tyr and (D)Leu-(D)Leu-(D)Tyr crystals, were chosen as candidates for modeling studies. The polar crystals of (L)Leu-(L)Leu-(L)Tyr form as well-developed {001} plates, delimited by faces from the {*hk*0} family in the *a* direction, {01̄1} faces in the $-b$ direction, and the (010) face in the $+b$ direction. The crystals of (D)Leu-(D)Leu-(D)Tyr develop enantiomorphous morphology by definition and in practice. Antibody 48E interacts exclusively with the (011) face of the (L)Leu-(L)Leu-(L)Tyr crystals, whereas antibody 602E interacts with the (011) face and with all the peripheral {*hk*0} faces of both (L)Leu-(L)Leu-(L)Tyr and (D)Leu-(D)Leu-(D)Tyr crystals.[18] The sequences of the variable regions of these two antibodies were determined and aligned to the sequences of antibody variable regions whose X-ray structures were previously ascertained. The structures of their variable domains were modeled using the structures of antibodies with high sequence similarity as templates and based on additional considerations described in detail below.

Antibody Sequencing

The total RNA was extracted from hybridoma cells and cDNA was obtained by reverse transcription. The genes of the heavy and light chain variable domains were amplified by the PCR and sequenced. The amino acid sequences of the variable domains of antibodies 48E and 602E are given in Table I.[25,37,38] Both the L1 and H3 loops of antibody 48E are considerably long (12 and 18 amino acid residues, respectively). In contrast, antibody 602E has shorter L1 (7 residues) and H3 (11 residues) loops. A high percentage of hydrophilic residues is prominent in the CDRs of antibody 48E, where serines and tyrosines constitute almost 50% of the CDR residues. In antibody 602E, four charged residues are prominent in the CDR loops (Lys L50, Arg H31, Arg

TABLE I. Amino Acid Sequences of Antibodies 48E and 602E

Light Chains

```
          1         10        20        30abcef31     40        50
48E       DTVVTQSPLSLPVSFGDQVSISCRSSQSLASSYGNTYLSWYLHKPGQSPQLLIYGISNRFSGV
602E      ----TQSPSSLSASLGDTITITCHASQNIN-----VWLSWYQQKPGNIPKLLIYKASNLHTGV
           60        70        80        90       100
48E       PDRFSGSGSGTDFTLKISTIKPEDLGMYYCLQGTHQPPTFGAGTKLELK
602E      PSRFSGSGSGTGFTLTISSLQPEDIATYYCQQGQSYPLTFGGGTKLEIK
```

Heavy Chains

```
          1         10        20        30        40        50 52a      60
48E       QVQLQESGAELVRSGASVKMSCKASGYTFTSYNMHWVKQTPGQGLEWIGYIYPGNGGTN YNQ
602E      QVQLQQSPGPLVAPSQSLSLTCTVSGFSLSRYSVHWVRQPPGKGLEWLGMIW-GGGSTDY NS
               70          80 82abc     90       100abcde        110
48E       KFKGKATLTADTSSSTAYMQISSLTSEDSAVYFCARGPIYYGSSLYFDYWGQGTTLTVSS
602E      ALKSRLSISKDNSKSQVFLKMNSLQTDDTAMYYCASYRYDGYYAM--DYWGQGTLVTVSS
```

The amino acid numbering and CDR positioning is according to Chothia et al.[25,37] and Al-Lazikani et al.[38]

H96, Asp H98). On the basis of the existing library, neither of the sequences is germline.

Antibody Modeling and Docking

Templates for modeling the light and heavy chains of each antibody were initially selected based on sequence comparison. As the relative juxtaposition of the heavy and light chain frameworks is an important factor for the structure of the binding site, preference was given to templates that matched both light and heavy chains. Finally, templates were selected where the canonical loops had the same length and sequence as the modeled antibody (see details below). The initial models (see Materials and Methods section) were energy minimized, keeping all the Cα atoms of the heavy and light chains fixed, except the H3 loop. The conformation of the H3 loop, which does not have a canonical structure, was modeled without backbone or side chain constraints.

Docking of the antibody models onto the different crystal faces was performed using the MolFit program.[32,33] The docked molecules are treated as rigid bodies and matching of the molecular surfaces is achieved by rotating and translating one molecule relative to the other and evaluating the degree of surface complementarity for each position on a relative scale.

Modeling Antibody 48E

One template for antibody 48E (1EHL) was used for modeling the framework of the heavy and light chains and for the L1, L2, H1, and H2 loops. Template 1EHL has 88% sequence identity to the 48E light chain and 72% sequence identity to the 48E heavy chain. Both the L3 and H3 loops are longer in antibody 48E than in 1EHL. Therefore, another template (1LMK), in which both the L3 and H3 loops are of the same length as in antibody 48E, was used to model these loops. Because the H3 loop is long, we expected that its predicted conformation would be considerably less reliable then the rest of the model structure. However, the experimental structures of the antibodies indicate that the H3 loop is delimited by the space occupied by the L1 and L3 loops, with which it forms extensive contacts.[39,40] The same template was therefore used for the H3 and L3 loops. Furthermore, the L1 loop of 1LMK has the same length as that of antibodies 48E and 1EHL, and it occupies the same region in space. Superposition of the Cα atoms of the 1EHL and 1LMK frameworks shows that they are similar, that is, the root mean square deviation (RMSD) is 0.6 Å. In particular, the interface between the heavy and light chains is very similar in the two structures.

The model structure of antibody 48E is presented in Figure 1. The recognition site of antibody 48E is composed of a high ridge formed by the L1 and H3 loops and a shallow groove formed by the L3, H1, and H2 loops. Among the residues exposed at the binding site there is a high percentage of serine (8) and tyrosine (5) residues, as well as asparagines (3), glutamines (2), glycines (5), threonines (2), histidine (1), isoleucines (2), and an alanine (1). The antigen binding surface of antibody 48E is mostly hydrophilic, with no charged residues.

Docking of Antibody 48E Onto Crystal Faces

The topography of the antigen recognition site of antibody 48E is dominated by the ridge formed by the long L1 and H3 loops. Considering that the predicted structure of the H3 loop is less reliable than that of the L1 loop, five residues in the apex of the H3 loop (Ile 97–Ser 100a) were omitted in the docking search. These residues were later added to each of the putative docking solutions and minimized in situ.

Antibody 48E was docked as described earlier onto each of the (011), (001), and (110) faces of (L)Leu-(L)Leu-(L)Tyr crystals and the (011) face of (D)Leu-(D)Leu-(D)Tyr crystals. For each crystal face, one or more model structures of putative complexes between the antibody and that face were obtained.

The crystal structure of (L)Leu-(L)Leu-(L)Tyr has been described in depth previously.[18] We thus limit the description here to the structure of the crystal surfaces to which docking was performed. Notably, the exposed crystal surfaces are in dynamic equilibrium with the solution, with molecules constantly attaching and detaching from the

surface. Which lattice sites will or will not be occupied at a given moment in time at a given surface depends on the interactions holding the molecule to the surface and on the interactions of the surface site with the solvent. Although a crystal face appears homogenous macroscopically, it almost certainly contains an average of these populations. The real structure of each crystal face may thus comprise different local structures, all pertaining to the same crystallographic plane, but having different structural and stereochemical features. To overcome this problem, the docking scans were performed on surfaces that comprised different regions, representing different local structures of the relevant face, which are likely to bind the antibody.

The (011) face of (L)Leu-(L)Leu-(L)Tyr is a good example of the above argument: at the surface, two crystallographically independent molecules emerge, which we marked 1 and 2 for convenience. We argued that the probability of having molecule 2 locally exposed at the (011) face is low. With molecule 2 present, the flat surface is favored in lattice energy but it is very hydrophobic. We thus estimate that, in water, the face will instead expose an undulating surface with exposed ammonium and carboxylate groups, as well as tyrosine hydroxyls in the grooves, whereas the ridges expose the carboxylate group and the side chain of only one leucine residue (Fig. 2).[18]

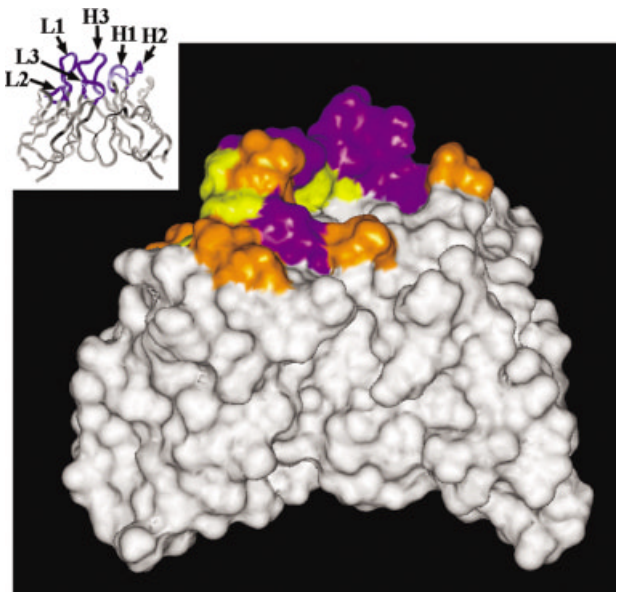

Fig. 1. A surface representation of the initial model of antibody 48E. Residues exposed at the binding site are colored: (orange) polar residues (S, Q, N, T), (yellow) hydrophobic residues (G, A, I), (purple) aromatic residues (Y, H). (Insert) A ribbon diagram of the initial model of antibody 48E. CDR loops are colored blue and labeled.

Docking of the model of antibody 48E onto the $(0\bar{1}1)$ face of the (L)Leu-(L)Leu-(L)Tyr crystals yielded two good solutions [Fig. 3(a and b)]. They differ in the orientation of the antibody relative to the crystal face, which is rotated by approximately 180° around its pseudo twofold axis. The MolFit complementarity scores for these solutions are similar (623 and 597 arbitrary score units). The difference between them (26 score units) is smaller than the σ for this scan (38 score units). It is notable that all the solutions in the top 2σ range of scores are variants of the solutions, differing one from the other only in the translation of the antibody along the crystal axes. Both docking models show astounding structural complementarity between the antibody and the crystal face. In both cases, the ridge of the antibody (loops L1 and H3) fits into the groove in the $(0\bar{1}1)$ crystal face and the groove of the antibody embraces the ridge of the crystal face. The buried surface area of the interface between the antibody and the $(0\bar{1}1)$ faces is approximately 1500 $Å^2$ in either of the two models. Note that each complex was energy minimized to optimize interactions; therefore, the conformation of the H3 loop is different for the antibodies in the two complexes, as are the side chain conformations. The complementarity scores for the optimized complexes (845 and 805) are higher than the initial scores because of the new contacts formed via the H3 loop. However, they are similar to each other, so that neither of the solutions can be eliminated.

Geometrically, the two sides of the groove of the $(0\bar{1}1)$ face are similar in that both sides fashion rather flat "walls," which run perpendicular to the groove (Fig. 2). Chemically, the groove exposes a leucine side chain of

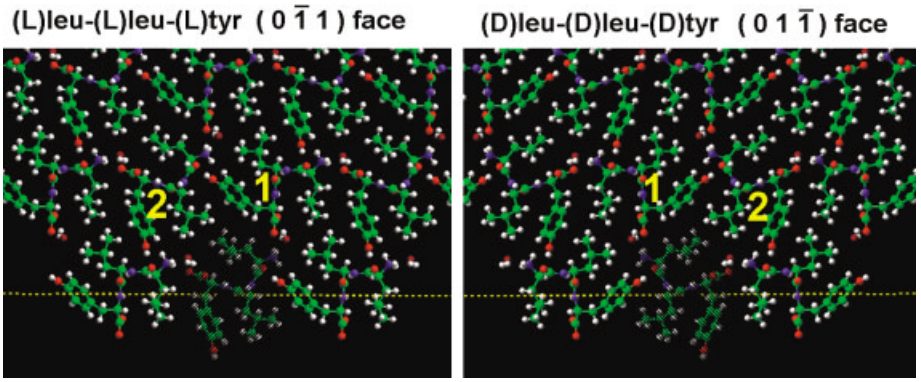

Fig. 2. Crystal packing of (left) (L)Leu-(L)Leu-(L)Tyr and (right) (D)Leu-(D)Leu-(D)Tyr as viewed edge-on to the $(0\bar{1}1)$ and $(01\bar{1})$ faces, respectively. Molecules of type 2 that are not likely to be exposed at the surface are drawn with broken lines. (White) hydrogen atoms, (red) oxygen atoms, (blue) nitrogen atoms, (green) carbon atoms.

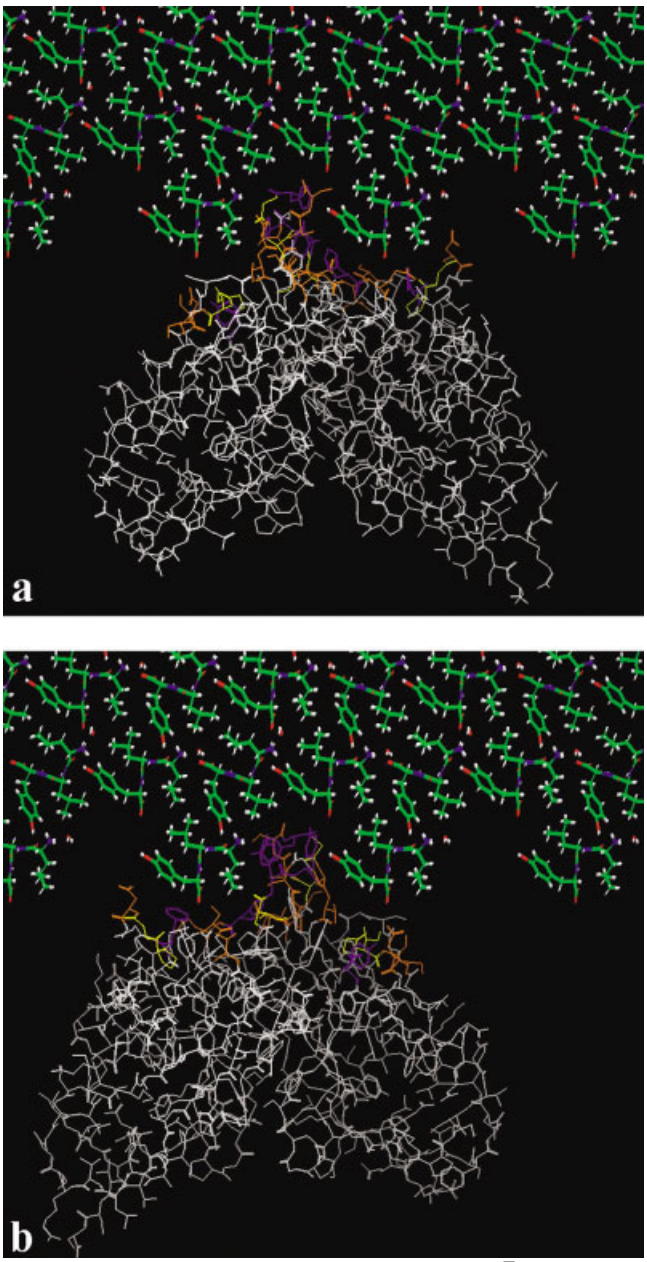

Fig. 3. Docking models of antibody 48E on the (011) face of the (L)Leu-(L)Leu-(L)Tyr crystal. Crystals: (white) hydrogen atoms, (red) oxygen atoms, (blue) nitrogen atoms, (green) carbon atoms. Antibodies: only residues exposed at the binding site are colored: (orange) polar residues (S, Q, N, T), (yellow) hydrophobic residues (G, A, I), (purple) aromatic residues (Y, H).

molecule 2, as well as the carboxy terminus and a part of the tyrosine ring of molecule 1. The amino terminus and the leucine side chain of molecule 1 are exposed at the left-hand side of the groove, whereas the leucine and tyrosine side chains of the next peptide molecule 1 are exposed at the right-hand side of the groove (Fig. 2). The geometric symmetry of the groove enables docking of the antibody in the two orientations. The different chemistry, however, implies different interactions between the antibody and the crystal in the two putative complexes. Possible interactions between the antibody and each surface were determined by measuring the distance between relevant atoms. Table II summarizes the contacts between the antibody and the (011) face of (L)Leu-(L)Leu-(L)Tyr crystals in the putative complexes. The dominant interactions are emphasized. In both cases binding is achieved via hydrogen bonding and hydrophobic interactions. In the first complex [Fig. 3(a)] there are 11 hydrogen bonds (4 dominant) and 10 hydrophobic interactions (2 dominant) whereas in the second complex [Fig. 3(b)] there are 12 hydrogen bonds (5 dominant) and 9 hydrophobic interactions (2 dominant). The expected differences in affinity are insignificant; hence, for both docking models, similar strong binding between the antibody and the crystal face should be established.

The (011) face of the (D)Leu-(D)Leu-(D)Tyr crystals is the mirror image of the (011) face of its enantiomer, which is the (L)Leu-(L)Leu-(L)Tyr crystal (Fig. 2). Thus, the two faces are identical chemically, expose the same functional groups, but differ in the orientation of the molecules relative to the surface. Docking of the model of antibody 48E onto the (011) face of (D)Leu-(D)Leu-(D)Tyr crystals yielded two solutions [Fig. 4(a and b)] in which the orientations of the antibody are similar to those obtained for the (011) face of the (L)Leu-(L)Leu-(L)Tyr crystal [Fig. 3(a and b)]. The equivalent juxtaposition of the antibody to each of the two enantiomeric surfaces is reflected by the MolFit scores, which differ by less than 1σ, implying a similar level of topographic complementarity. The most obvious difference in the binding site conformation is in the H3 loop; this adopts, in both complexes with the (D)Leu-(D)Leu-(D)Tyr crystal face, a conformation in which tyrosines H98 and H99 are rotated toward each other and are thus less available for binding the crystal face.

In contrast to the similarities in geometric complementarity between the two enantiomers, the chemistry of the recognition between antibody 48E and the two enantiomeric faces is fundamentally different. There are significantly fewer interactions of the antibody with the (011) face of (D)Leu-(D)Leu-(D)Tyr than with the (011) face of (L)Leu-(L)Leu-(L)Tyr, in both orientations. There are 6 hydrogen bonding interactions (2 dominant) and 7 hydrophobic interactions (2 dominant) in the first complex with the (D)Leu-(D)Leu-(D)Tyr crystal face [Fig. 4(a) and Table II] as opposed to 11 and 10 interactions, respectively, in the complex with the (L)Leu-(L)Leu-(L)Tyr surface [Fig. 3(a) and Table II). In the second complex with the (D)Leu-(D)Leu-(D)Tyr face [Fig. 4(b)] there are 10 hydrogen bonding interactions (3 dominant) and 5 hydrophobic interactions (2 dominant) as opposed to 12 and 9 corresponding contacts, respectively, in the complex with the (L)Leu-(L)Leu-(L)Tyr surface [Fig. 3(b) and Table II].

The tripeptide crystals contain water molecules that are part of the crystal lattice. The antibody molecule was therefore docked onto crystal faces that expose surfaces with and without the water molecules. It is interesting that the optimal docking solution onto the (L)Leu-(L)Leu-(L)Tyr (011) face was obtained using the crystal surface without water molecules, whereas the optimal docking

TABLE II. Contacts Between Antibody 48E and Crystals of (L2)leu-(L)leu-(L)tyr and (D)leu-(D)leu-(D)tyr

CDR	Residue	L-Complex 1[a]	D-Complex 1[b]	L-Complex 2[c]	D-Complex 2[d]
L1	Alanine L30/Cβ	Leucine CH_3 (LR)	—	—	—
	Serine L30a/OH	**Tyrosine —OH (RR)[e]**	—	—	—
	Serine L30b/NH	**Tyrosine —OH (RG)[e]**	Tyrosine —OH (RG)	—	—
	Serine L30b/CH_2	—	—	Leucine CH_3 (LG)	Leucine CH_3 (LG)
	Serine L30b/OH	**Tyrosine —OH (RG)[e]**	—	**NH_3^+ terminus (I)[e]**	**NH_3^+ terminus (I)[e]**
	Serine L30b/OH	**COO^- terminus (I)[e]**	**COO^- terminus (I)[e]**	—	—
	Tyrosine L30c/OH	Tyrosine —OH (RG)	**Tyrosine —OH (RG)[e]**	**NH_3^+ terminus (I)[e]**	**NH_3^+ terminus (I)[e]**
	Tyrosine L30c/OH	COO^- terminus (I)	—	—	—
	Tyrosine L30c/CH	Tyrosine CH (I)	Tyrosine CH (I)		
	Tyrosine L30c/C═O	NH_3^+ terminal (LG)	H_2O (I)	—	—
	Glycine L30e/Cα	—	—	Leucine CH_3 (RG)	—
	Glycine L30e/C═O	NH_3^+ terminal (LG)	—	Tyrosine OH (RG)	Tyrosine OH (RG)
	Asparagine L30f/Cα	Leucine CH_3 (LR)	Leucine CH_3 (LR)	—	—
	Threonine L31/Cβ	Leucine CH_3 (LR)	**Leucine CH_3 (LR)[e]**	Tyrosine ring CH (RG)	Tyrosine ring CH (RG)
	Threonine L31/OH	—	—	Tyrosine OH (RG)	—
L2	Asparagine L53/Nδ	COO^- terminus (LR)	COO^- terminus (LR)	COO^- terminus (RR)	COO^- terminus (RR)
L3	Histidine L93/ring	**Tyrosine ring (RR)[e]** "herring-bone"	Tyrosine ring (RR) "herring-bone"	Leucine CH_3 (LG)	**Leucine CH_3 (LG)[e]**
	Glutamine L94/Nε	COO^- terminus (RR)	COO^- terminus (RR)	COO^- terminus (LR)	COO^- terminus (LR)
	Glutamine L94/NH	—	—	COO^- terminus (LR)	COO^- terminus (LR)
H1	Serine H31/OH	—	—	**COO^- terminus[e] (LR)**	**COO^- terminus (LR)[e]**
H2	Tyrosine H50/OH	—	—	**COO^- terminus[e] (LR)**	COO^- terminus (LR)
	Tyrosine H52/ring CH	Leucine CH_3 (RR)	—	Tyrosine ring CH (LR)	Tyrosine ring CH (LR)
	Glycine H53/Cα	Leucine CH_3 (RR)	—	—	—
	Asparagine H54/Cβ	Leucine CH_3 (RR)	Leucine CH_3 (RR)	—	—
H3	Isoleucine H97/Cα	—	—	Leucine CH_3 (LG)	—
	Tyrosine H98/Cβ	**Tyrosine ring CH (I)[e]**	**Tyrosine ring (I)[e]**	**Leucine CH_3 (LG)[e]**	**Leucine CH_3 (LG)[e]**
	Tyrosine H98/OH	—	—	NH_3^+ terminus (LG)	—
	Tyrosine H99/ring CH	—	—	**Tyrosine ring CH[e] (I)**	—
	Tyrosine H99/OH		—	**COO^- terminus (I)[e]**	COO^- terminus (I)
	Serine L67/OH	COO^- terminus (LR)	—	COO^- terminus (I)	COO^- terminus (I)
	Glycine L68/Cα	Leucine CH_3 (LR)	Leucine CH_3 (LR)	Tyrosine CH (RG)	—

The contacts were determined as follows: < 4.0 Å for hydrogen bonds and <4.5 Å for hydrophobic contacts. LR, left-hand side ridge; RR, right-hand side ridge; RG, right-hand side of groove; I, inside groove; LG, left-hand side of groove.
[a]Figure 3(a).
[b]Figure 4(a).
[c]Figure 3(b).
[d]Figure 4(b).
[e]Dominant interactions include buried hydrogen bonds with good geometry (<3.5 Å) and multiple residue–residue hydrophobic contacts.

onto the (D)Leu-(D)Leu-(D)Tyr ($01\bar{1}$) face was obtained using the surface with water molecules. Indeed, water molecules are involved in the interactions between antibody 48E and the (D)Leu-(D)Leu-(D)Tyr (011) face (Table II).

The two possible complexes between antibody 48E and the (L)Leu-(L)Leu-(L)Tyr (011) face provide equally good fits both geometrically (Fig. 3) and chemically (Table II). The two possible complexes between the antibody and the (D)Leu-(D)Leu-(D)Tyr ($01\bar{1}$) face are also roughly equivalent to each other (Fig. 4 and Table II). However, both complexes of the antibody with the (L)Leu-(L)Leu-(L)Tyr (011) face are significantly more favorable than those with the (D)Leu-(D)Leu-(D)Tyr ($01\bar{1}$) face in terms of chemical interactions. This favored chemical interaction matches the experimental results well,[18] namely, antibody 48E recognizes the (011) face of (L)Leu-(L)Leu-(L)Tyr, but not the ($01\bar{1}$) face of (D)Leu-(D)Leu-(D)Tyr.

The (001) face of (L)Leu-(L)Leu-(L)Tyr crystals is also an undulating surface. The ridges expose the methyl groups of one leucine residue and the carboxylate group of the peptide molecule whereas the grooves expose the methyl groups of the second leucine residue of the same molecule and the aromatic tyrosine ring of the second molecule. Docking of the model of antibody 48E to the (001) face of (L)Leu-(L)Leu-(L)Tyr crystals (Fig. 5) shows significantly poorer shape complementarity than on the (011) face. The relatively shallow and wide groove does not permit close contact of the antibody and the crystal surface, resulting in a significantly smaller interface area (~1100 $Å^2$).

All {*hk*0} have similar structural characteristics and stability; thus, they have a tendency to interchange and combine [(110)–(120), etc.].[18] The (110) face was taken as a representative of the {*hk*0} family. The (110) face exposes the main chain of the peptide almost entirely. In particular, the amino terminus and the two leucine residues of one peptide molecule, as well as the amino terminus, one leucine residue, and amide carbonyl moieties of the second peptide molecule, are exposed. This face is flat, as are all {*hk*0} faces. However, taking into account the possible local

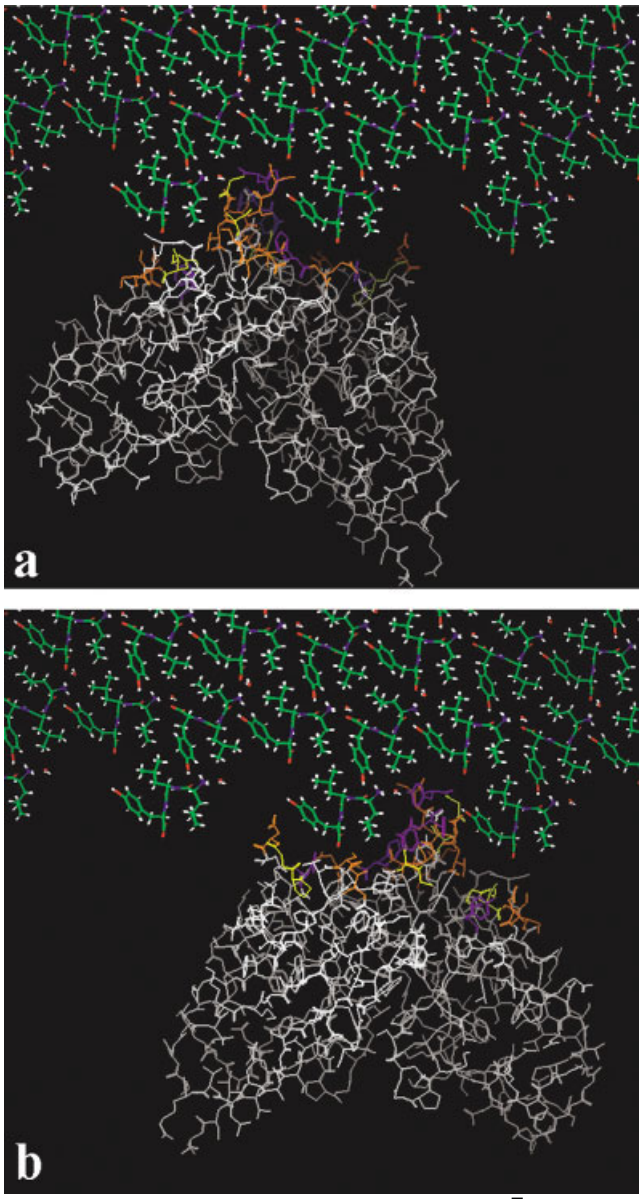

Fig. 4. Docking models of antibody 48E on the (01$\bar{1}$) face of the (D)Leu-(D)Leu-(D)Tyr crystal. Crystals: (white) hydrogen atoms, (red) oxygen atoms, (blue) nitrogen atoms, (gray) carbon atoms. Antibodies: only residues exposed at the binding site are colored: (orange) polar residues (S, Q, N, T), (yellow) hydrophobic residues (G, A, I), (purple) aromatic residues (Y, H).

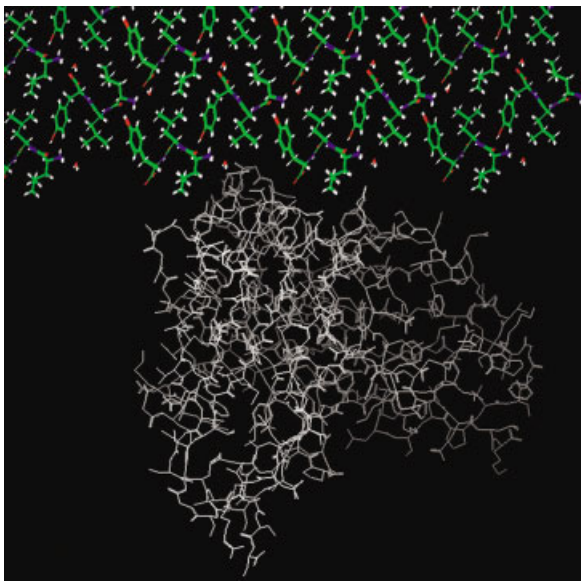

Fig. 5. The docking model of antibody 48E on the (001) face of the (L)Leu-(L)Leu-(L)Tyr crystal. Crystals: (white) hydrogen atoms, (red) oxygen atoms, (blue) nitrogen atoms, (green) carbon atoms. Antibody is white.

differences, as discussed above, we have removed one molecule from the surface of the (110) face at one site, so that a local groove is formed. Even if this groove is present with a low probability, it would enable a better fit to the binding site of antibody 48E than the more abundant flat regions of the face. Nevertheless, docking of the model of antibody 48E to the (110) face of (L)Leu-(L)Leu-(L)Tyr crystals (Fig. 6) did not yield any solution that involves significant CDR interactions with the crystal face. Residues that are not in the antibody's antigen recognition site dominate the interactions between the antibody and the crystal face in all solutions. In the light of the current knowledge of antibody–antigen binding, such antibody binding is unlikely. Manual docking of antibody 48E to the (110) face of (L)Leu-(L)Leu-(L)Tyr crystals shows a possible model for an interaction between the antibody and the surface, involving CDR residues. It is evident that such an interaction allows less burial of the antibody surface than in the (01$\bar{1}$) docking models (Fig. 3) and fewer favorable chemical interactions.

Modeling Antibody 602E

For antibody 602E we used one template (1IGT) for the modeling of the light chain, including the CDRs, and another template (1IBG) was used for the framework of the heavy chain and for the H1 and H2 CDRs. A third template (1FVC) was used for modeling the H3 loop. There is 100% sequence identity between the light chains of 1IGT and 602E and 82% sequence identity between the heavy chains of 1IBG and 602E. These two templates also display a high sequence similarity of the heavy and light chain interface residues, as well as similar juxtaposition of the heavy and light chains (RMSD = 0.57 Å).

The classification of H3 conformations, as described by Morea and coworkers,[26] correlates between a bulged H3 conformation and the presence of an arginine residue in position 94, as well as an aspartic acid residue in position 101. The ionic interaction between these residues is considered crucial for stabilizing the bulged conformation. Antibody 602E does not have an arginine in position 94. Nevertheless, its H3 loop was built in a bulged conformation based on the structure of PDB entry 1FE8,[31,41] in which the H3 loop shows high sequence similarity to the H3 loop in antibody 602E. In 1FE8, the bulged conformation of the H3 loop is stabilized by hydrogen bonding of the aspartic acid residue in position 101 to the backbone NH of

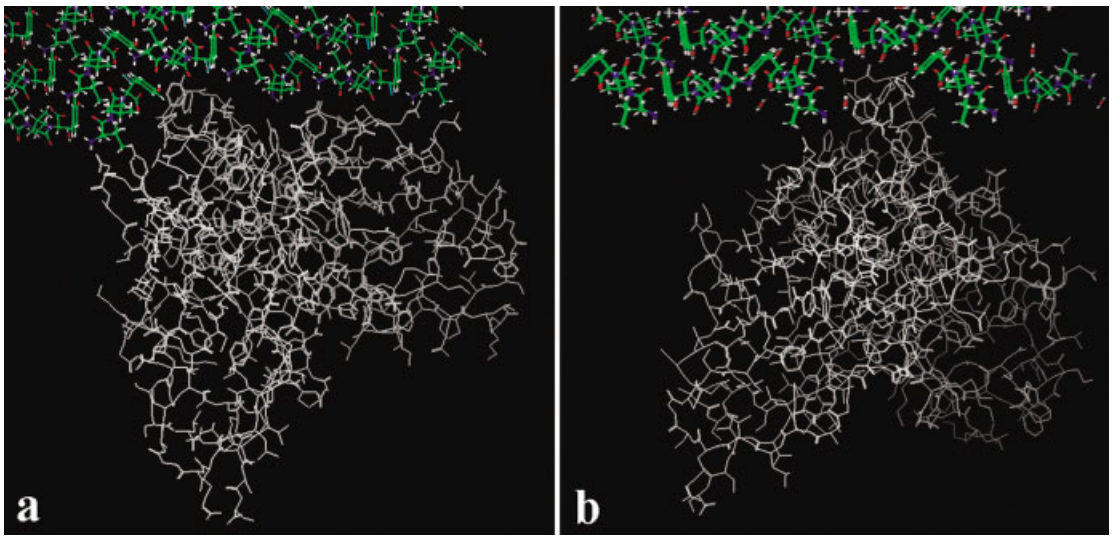

Fig. 6. Docking models of antibody 48E on the (110) face of (L)Leu-(L)Leu-(L)Tyr crystals. (**a**) Automatic docking solution and (**b**) manual docking. Crystals: (white) hydrogen atoms, (red) oxygen atoms, (blue) nitrogen atoms, (green) carbon atoms. Antibodies are white.

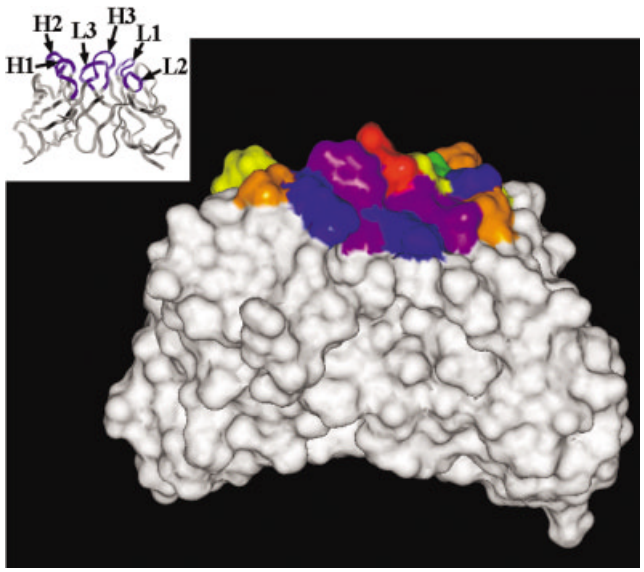

Fig. 7. A surface representation of the initial model of antibody 602E. The residues exposed at the binding site are colored: (blue) positively charged residues (R, K), (red) negatively charged residues (D), (orange) polar residues (S, Q, N, T), (yellow) hydrophobic residues (G, A, I), (green) tryptophans, (purple) tyrosines and histidine residues. (Insert) A ribbon diagram of the initial model of antibody 602E. The CDR loops are colored blue and labeled.

the glycine residue in position 100b. In our model the bulged conformation of the H3 loop is stabilized by a similar hydrogen bond between the aspartic acid residue in position 101 and the backbone NH of the alanine in position 100b.

The model of antibody 602E is presented in Figure 7. The antigen recognition site of 602E is rather flat, exposing four charged residues: 2 arginines, 1 lysine, and 1 aspartic acid, in addition to asparagines (3), glutamine (1), glycines (2), threonine (1), tyrosines (2), tryptophan (1), isoleucine (1), and leucine (1).

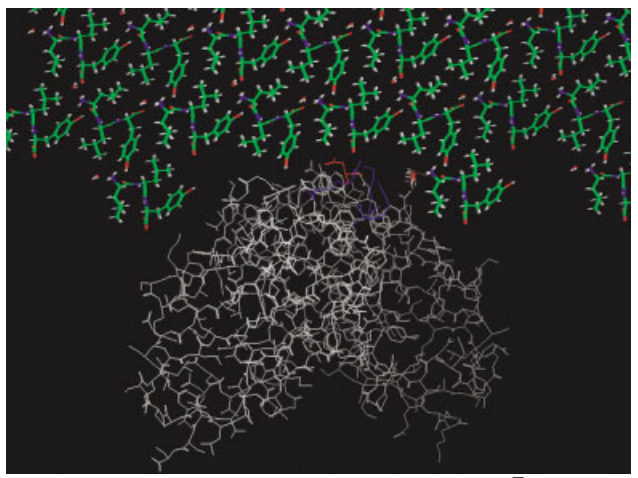

Fig. 8. The docking model of antibody 602E onto the $(0\bar{1}1)$ face of the (L)Leu-(L)Leu-(L)Tyr crystals. Residues exposed at the binding site are colored. Crystals: (white) hydrogen atoms, (red) oxygen atoms, (blue) nitrogen atoms, (green) carbon atoms. Antibody residues exposed at the binding site are colored: (blue) positively charged residues (R, K), (red) negatively charged residues (D), (orange) polar residues (S, Q, N, T), (yellow) hydrophobic residues (G, A, I), (light green) tryptophans, (green) tyrosines and histidine residues.

Docking of Antibody 602E Onto Crystal Faces

Antibody 602E was docked (as described in the Experimental section) onto each of the $(0\bar{1}1)$, (001), and (110) faces of (L)Leu-(L)Leu-(L)Tyr crystals.

Docking of antibody 602E onto the $(0\bar{1}1)$ and $\{hk0\}$ faces shows shape complementarity to the flat regions of these faces (Fig. 8), burying ~1200 Å^2. As discussed above, the $(0\bar{1}1)$ face of (L)Leu-(L)Leu-(L)Tyr crystals in water is expected to consist mostly of a ridge and groove motif. However, flat regions may be exposed on these surfaces as a result of the equilibrium interchange between the surface molecules and molecules in the solution. Interactions

between the flat binding site of the antibody and flat regions on the crystal surfaces are dominated by electrostatic attraction. At least two of the four charged residues at the antibody binding site are engaged in electrostatic interactions with charged moieties on the crystal faces. On the (011) face, arginines H31 and L46 are in close proximity to the carboxy termini of the tripeptide molecules. On the (110) face, arginine H31 interacts with the carboxy terminus of a peptide molecule and aspartic acid L101 interacts with the amino terminus of a peptide molecule (not shown). These electrostatic interactions presumably stabilize the binding of the antibody to these crystal faces. The wavy topography of the (001) face prevents good complementarity with the flat binding surface of antibody 602E.

DISCUSSION

The structural basis of antibody-surface recognition was studied in a system involving antibodies selected by their recognition of crystals of the tripeptide (L)Leu-(L)Leu-(L)Tyr.

The variable regions of two antibodies were cloned and sequenced. Structural models of their variable domains were built, based on sequence similarity to antibodies whose X-ray structures are known. Docking of the antibody models on the different crystal faces of (L)Leu-(L)Leu-(L)Tyr and (D)Leu-(D)Leu-(D)Tyr was then performed using MolFit,[32,33] which estimates the geometric fit between two surfaces, in order to maximize the contact surface complementarity. The docking results are interpreted and compared with the experimental results on binding selectivity vis-à-vis the different crystal faces of the same crystal and the enantiomorphous crystal faces of the enantiomeric crystals. Specifically, antibody 48E is enantioselective and surface selective for the (01$\bar{1}$) face of (L)Leu-(L)Leu-(L)Tyr. Antibody 602E is not enantioselective and has low surface selectivity.[18]

The face specificity exhibited by antibody 48E is attributed to the prominent differences in the structural complementarity between the antibody and the different crystal faces. The stereoselectivity of the antibody is visually and computationally self-evident from the models of the antibody docked onto the different crystal faces. The topographical differences between the various crystal surfaces are well resolved, and the antibody detects them. The chiral discrimination manifested by this antibody is nevertheless not obvious, because the overall geometric features (ridge–groove motif) and the chemical characteristics of the surfaces are preserved in both enantiomer crystals.[18] The expression of chirality on the (011) face is detectable in the different orientation of the peptide stacking relative to the overall geometrical features (ridges and grooves) of the surface. The fact that the antibody can discriminate between the enantiomeric surfaces, in spite of their topographic similarity (Fig. 2), is an impressive demonstration of the recognition power of the immune system. This enantioselectivity is not, however, immediately evident from inspection of the docking models.

The docking procedure yielded two solutions for the docking of antibody 48E on the (01$\bar{1}$) faces of (L)Leu-(L)Leu-(L)Tyr. The two solutions are related by a pseudo twofold rotation of the antibody relative to the crystal groove (Fig. 3). The two components are thus juxtaposed such that the same antibody surface faces the tyrosine-lined side of the groove in one model and the leucine side in the other. The docking program ranks the two solutions as being of similar quality, because it accounts only for steric matching, independent of the nature of the interactions arising between the groups in contact. Two similar solutions were obtained for docking of antibody 48E onto the (01$\bar{1}$) face of (D)Leu-(D)Leu-(D)Tyr crystals (Fig. 4). The geometric complementarity in the complexes with the (D)Leu-(D)Leu-(D)Tyr crystals is similar to that of the complexes with the (011) face of (L)Leu-(L)Leu-(L)Tyr crystals. Extremely tight packing between the antibody and the crystal characterizes all suggested docking models, intuitively hinting at the possibility of chiral discrimination. Indeed, a detailed analysis of the possible interactions between the antibody and the crystal face shows that many more favorable interactions may ensue in the docking models between the antibody and the (L)Leu-(L)Leu-(L)Tyr crystal than with the (D)Leu-(D)Leu-(D)Tyr crystal. The combination of the computerized geometric docking with manual examination of the results, accounting for chemical considerations, thus provides a complete picture of the binding and recognition potential of the antibody, which is in agreement with the experimental results. An experimental validation of the importance of the suggested interactions could conceivably be provided by site-directed mutagenesis. Unfortunately, this is not possible in the present case, nor in all cases of antibodies interacting with crystal surfaces, which are all of the IgM subtype so far. The cooperative interactions of the intact antibody with the repetitive epitopes on the crystal surface appears to be essential to binding. Thus, binding of isolated $F(Ab)_2$ fragments was found to be at least 1 order of magnitude lower than that of the intact IgM. Measuring the binding of Fv fractions after mutagenesis thus becomes nearly impossible.

In the case of antibody 602E, binding to the (0$\bar{1}$1) and {hk0} faces on both the (L)Leu-(L)Leu-(L)Tyr and (D)Leu-(D)Leu-(D)Tyr crystals appears to be driven by electrostatic interactions, overriding topographic complementarity. The lower face selectivity exhibited by this antibody, as well as its lack of chiral discrimination, are interpreted with a similar rationale, namely, that ionic interactions are individually stronger than other interactions, such as van der Waals interactions. They are also much more permissive in the requirements of complementarity between interacting partners.

The fact that antibody 602E has four charged residues in the binding site, but antibody 48E does not have any, is thus important for understanding the difference in their level of specificity. In the case of antibody 48E, the contact area between the antibody and the crystal face it binds is very large (1500 Å^2), because of the extensive topographical complementarity between the two surfaces. In addi-

tion, many chemical interactions arise from chemical complementarity between the surfaces. The accumulation of these interactions over such a large area is expected to result in high binding enthalpy and thus strong binding of the antibody to the crystal face. On other crystal faces, where the topographical complementarity is not as good, fewer chemical interactions are possible, resulting in low binding enthalpy and no binding of the antibody to the surfaces. In the case of antibody 602E, the presence of charged residues at the binding site enables binding of the antibody to various surfaces, even when the topographical complementarity between the surfaces is not very good and there is lower contact area between the surfaces.

A similar scenario was observed previously for antibodies 36A1 and 23C1, which were raised and selected against crystals of cholesterol monohydrate and *p*-dinitrobenzene, respectively.[27] Antibody 36A1 was shown to preferentially bind one specific crystal face, whereas antibody 23C1 is a cross-reactive antibody that binds to high energy sites on various surfaces. The comparison of the two antibodies was made easier and the implications were even more striking in this latter case, because the amino acid sequences of the variable regions of the two antibodies have 91% identity. The models of the binding sites were consequently quite similar. However, antibody 23C1 has four charged residues exposed in its binding site, whereas the binding site of antibody 36A1 exposes no charged residues. It is thus confirmed that lack of specificity in antibodies that bind surfaces may be induced by the presence of charged residues in their binding site, whereas extensive chemical and structural complementarity over large areas fosters high levels of specificity.

It is well known and documented that antibody–antigen binding is based on a high degree of shape complementarity and chemical complementarity, including hydrophobic interactions, hydrogen bonding, and salt bridges.[42,43] Antibodies against hen egg-white lysozyme demonstrate increased affinity with the increase of the nonpolar buried surface.[44,45] However, the presence of charged residues is also correlated with increased affinity in antibody–protein binding,[46] as well as in antibody–hapten[47,48] and antibody–carbohydrate binding.[49,50] In the case of anti-double-strand DNA antibodies, the source of polyreactivity is in the interactions of charged groups in the binding site with the phosphate backbone of DNA. In contrast, specific recognition involves matching of complementary arrays of hydrogen bonds of the antibody with the specific DNA base sequence.[10] Increased affinity does not intuitively imply increased specificity; rather, the opposite would be expected, especially in the case of electrostatic interactions. Maturation of an antibody response leading to increased affinity may involve increased specificity[46,50,51] and altered specificity.[52] This is not the case, however, for IgM antibodies that do not undergo classical affinity maturation and thus are not subject to a directed increase in affinity and specificity. The antibodies selected and examined here are all IgM. Besides not undergoing maturation, the cooperative interactions of 10 binding sites on an extended surface such as that of a crystal are expected, by themselves, to increase the affinity of the binding at the expense of the specificity, if nonspecific charge interactions dominate. Within this framework, the lack of specificity of antibody 602E is not surprising. The exquisite stereo- and enantioselectivity of antibody 48E, and the mechanism underlying it, are certainly more interesting and surprising.

CONCLUSION

The interplay between molecular chirality, surface chirality, and molecular recognition was investigated in order to better understand the factors influencing antibody specificity. Modeling of antibody binding sites and of antibody–antigen complexes provided a rational framework for understanding the rules governing such specificity (or lack thereof).

The experimentally proven discrimination of antibody 48E for the enantiomorphous surfaces once again stressed the astounding level of molecular recognition that may be achieved in antibody–antigen complexes.[18] The binding site models and docking models of the respective complexes rationalize the experimental results, while demonstrating the power of the modeling techniques for predicting detailed antibody–antigen contacts.

ACKNOWLEDGMENTS

We thank Naama Kessler for helpful advice regarding the cloning and sequencing. Author (L.A.) is incumbent of the Dorothy and Patrick Gorman Professorial Chair and author (M.G.) is the recipient of the Jeaninne Klueger Scholarship. This work was supported by a grant from the Israel Science Foundation, administered by the Israel Academy of Sciences.

REFERENCES

1. Davies DR, Padlan EA, Sheriff S. Antibody–antigen complexes. Annu Rev Biochem 1990;59:439–473.
2. Branden C, Tooze J. Introduction to protein structure. New York: Garland; 1991.
3. Wilson IA, Stanfield RL. Antibody–antigen interactions: new structures and new conformational changes. Curr Opin Struct Biol 1994;4:857–867.
4. van Regenmortel MHV. From absolute to exquisite specificity. Reflections on the fuzzy nature of species, specificity and antigenic sites. J Immunol Methods 1998;216:37–48.
5. Arevalo JH, Taussig MJ, Wilson IA. Molecular basis of cross reactivity and the limits of antibody–antigen complementarity. Nature 1993;365:859–863.
6. Arevalo JH, Hassig CA, Stura EA, Sims MJ, Taussig MJ, Wilson IA. Structural analysis of antibody specificity. J Mol Biol 1994;241: 663–690.
7. Braden BC, Fields BA, Ysern X, Goldbaum FA, DallAcqua W, Schwarz FP, Poljak RJ, Mariuzza RA. Crystal structure of the complex of the variable domain of antibody D1.3 and turkey egg white lysozyme: a novel conformational change in antibody CDR-L3 selects for antigen. J Mol Biol 1996;257:889–894.
8. Notkins AL. Polyreactive antibodies and polyreactive antigen-binding B (PAB) cells. In: Potter M, Melchers F, editors. B1 lymphocytes in B-cell neoplasia. Current topics in microbiology and immunology. Volume 252. Berlin: Springer–Verlag; 2000.
9. James LC, Roversi P, Tawfik DS. Antibody multispecificity mediated by conformational diversity. Science 2003;299:1362–1367.
10. Ackroyd PC, Cleary J, Glick GD. Thermodynamic basis for sequence-specific recognition of ssDNA by an autoantibody. Biochemistry 2001;40:2911–2922.
11. Perl-Treves D, Kessler N, Izhaky D, Addadi L. Monoclonal anti-

body recognition of cholesterol monohydrate crystal faces. Chem Biol 1996;3:567–577.
12. Kessler N, Perl-Treves D, Addadi L. Monoclonal antibodies that specifically recognize crystals of dinitrobenzene. FASEB J 1996;10: 1435–1442.
13. Bromberg R, Kessler N, Addadi L. Antibody recognition of specific crystal faces of 1,4 dinitrobenzene. J Cryst Growth 1998;193:656–664.
14. Izhaky D, Addadi L. Pattern recognition of antibodies for two-dimensional arrays of molecules. Adv Mater 1998;10:1009–1013.
15. Izhaky D, Addadi L. Stereoselective interactions of a specialized antibody with cholesterol and epicholesterol monolayers. Chem Eur J 2000;6:869–874.
16. Geva M, Izhaky D, Mickus DE, Rychnovsky SD, Addadi L. Stereoselective recognition of monolayers of cholesterol, entcholesterol, and epicholesterol by an antibody. ChemBioChem 2001;2:265–271.
17. Geva M, Addadi L. Stereospecific and structure specific recognition of two- and three-dimensionally organized surfaces by biological macromolecules. Mol Cryst Liq Cryst 2002;390:57–66.
18. Geva M, Frolow F, Eisenstein M, Addadi L. Antibody recognition of chiral surfaces. The enantiomorphous crystals of leucine–leucine–tyrosine. J Am Chem Soc 2003;125:696–704.
19. Mylvaganam SE, Paterson Y, Getzoff ED. Structural basis for the binding of an anti cytochrome *c* antibody to its antigen: crystal structures of FabE8 cytochrome *c* complex to 1.8 angstrom resolution and FabE8 to 2.26 angstrom resolution. J Mol Biol 1998;281: 301–322.
20. Betts MJ, Sternberg MJE. An analysis of conformational changes on protein–protein association: implications for predictive docking. Protein Eng 1999;12:271–283.
21. Bossart-Whitaker P, Chang CY, Novotny J, Benjamin DC, Sheriff S. The crystal structure of the antibody N10-staphylococcal nuclease complex at 2.9 angstrom resolution. J Mol Biol 1995;253:559–575.
22. Rini JM, Schulzegahmen U, Wilson IA. Structural evidence for induced fit as a mechanism for antibody–antigen recognition. Science 1992;255:959–965.
23. Stanfield RL, Takimotokamimura M, Rini JM, Profy AT, Wilson IA. Major antigen induced domain rearrangements in an antibody. Structure 1993;1:83–93.
24. Kabat EA, Wu TT, Bilofsky H. Unusual distribution of amino acids in complementarity determining (hypervariable) segments of heavy and light chains of immunoglobulins and their possible roles in specificity of antibody-combining sites. J Biol Chem 1977;252:6609–6616.
25. Chothia C, Lesk AM, Tramontano A, Levitt M, Smith-Gill SJ, Air G, Sheriff S, Padlan EA, Davies D, Tulip W, Colman PM, Spinelli S, Alzari PM, Poljak RJ. Conformations of immunoglobulin hypervariable regions. Nature 1989;342:877–883.
26. (a) Morea V, Tramontano A, Rustici M, Chothia C, Lesk AM. Conformations of the third hypervariable region in the VH domain of immunoglobulins. J Mol Biol 1998;275:269–294; (b) Morea V, Lesk AM, Tramontano A. Antibody modeling: implications for engineering and design. Methods 2000;20:267–279.
27. Kessler N, Perl-Treves D, Addadi L, Eisenstein M. Structural and chemical complementarity between antibodies and the crystal surfaces they recognize. Proteins Struct Funct Genet 1999;34:383–394.
28. Orlandi R, Gussow DH, Jones PT, Winter G. Cloning of immunoglobulin variable domains for expression by the polymerase chain reaction. Proc Natl Acad Sci USA 1989;86:3833–3837.
29. Pearson WR, Lipman DJ. Improved tools for biological sequence comparison. Proc Natl Acad Sci USA 1988;85:2444–2448.
30. Pearson WR. Empirical statistical estimates for sequence similarity searches. J Mol Biol 1998;276:71–84.
31. Berman HM, Westbrook J, Feng Z, Gilliland G, Bhat TN, Weissig H, Shindyalov IN, Bourne PE. The Protein Data Bank. Nucleic Acids Res 2000;28:235–242.
32. Katchalski-Katzir E, Shariv I, Eisenstein M, Friesem AA, Aflalo C, Vakser IA. Molecular-surface recognition—determination of geometric fit between proteins and their ligands by correlation techniques. Proc Natl Acad Sci USA 1992;89:2195–2199.
33. Eisenstein M, Shariv I, Koren G, Friesem AA, Katchalski-Katzir E. Modeling supra molecular helices: extension of the molecular surface recognition algorithm and application to the protein coat of the tobacco mosaic virus. J Mol Biol 1997;266:135–143.
34. Ben-Zeev E, Berchanski A, Heifetz A, Shapira B, Eisenstein M. Prediction of the unknown: inspiring experience with the CAPRI experiment. Proteins Struct Funct Genet 2003;52:41–46.
35. Mendez R, Leplae R, De Maria L, Wodak SJ. Assessment of blind predictions of protein protein interactions: current status of docking methods. Proteins Struct Funct Genet 2003;52:51–67.
36. Levitt M, Gerstein M. A unified statistical framework for sequence comparison and structure comparison. Proc Natl Acad Sci USA 1998;95:5913–5920.
37. Chothia C, Lesk AM. Canonical structures for the hypervariable regions of immunoglobulins. J Mol Biol 1987;196:901–917.
38. Al-Lazikani B, Lesk AM, Chothia C. Standard conformations for the canomical structures of immunoglobulins. J Mol Biol 1997;273: 927–948.
39. Van Regenmortel MHV. Reductionism and the search for structure–function relationships in antibody molecules. J Mol Recognit 2002;15:240–247.
40. Ramsland PA, Farrugia W. Crystal structures of human antibodies: a detailed and unfinished tapestry of immunoglobulin gene products. J Mol Recognit 2002;15:248–259.
41. Romijn RAP, Bouma B, Wuyster W, Gros P, Kroon J, Sixma JJ, Huizinga EG. Identification of the collagen-binding site of the von Willebrand factor A3-domain. J Biol Chem 2001;276:9985–9991.
42. Roitt I. Essential immunology. Oxford, UK: Blackwell Scientific; 1991.
43. Sundberg EJ, Mariuzza RA. Molecular recognition in antibody–antigen complexes. In: Janin J, Wodak SJ, editors. Advances in protein chemistry. Volume 61. San Diego, CA: Academic; 2002. p 119–160.
44. Sundberg EJ, Urrutia M, Braden BC, Isern J, Tsuchiya D, Fields BA, Malchiodi EL, Tormo J, Schwarz FP, Mariuzza RA. Estimation of the hydrophobic effect in an antigen antibody protein–protein interface. Biochemistry 2000;39:15375–15387.
45. Li Y, Li H, Yang F, Smith-Gill SJ, Mariuzza RA. X-ray snapshots of the maturation of an antibody response to a protein antigen. Nature Struc Biol 2003;10:482–488.
46. Sinha N, Mohan S, Lipschultz CA, Smith-Gill SJ. Differences in electrostatic properties at antibody–antigen binding sites: implications for specificity and cross-reactivity. Biophys J 2002;83:2946–2968.
47. Livesay D, Linthicum S, Subramaniam S. pH Dependence of antibody:hapten association. Mol Immunol 1999;36:397–410.
48. Chong LT, Duan Y, Wang L, Massova I, Kollman PA. Molecular dynamics and free energy calculations applied to affinity maturation in antibody 48G7. Proc Nat'l Acad Sci 1999;96:14330–14335.
49. Muller-Loennies S, MacKenzie CR, Patenaude SI, Evans SV, Kosma P, Brade H, Brade L, Narang S. Characterization of high affinity monoclonal antibodies specific for chlamydial lipopolysaccharide. Glycobiology 2000;10:121–130.
50. Thomas R, Patenaude SI, MacKenzie CR, To R, Hirama T, Young NM, Evans SV. Structure of an anti-blood group A Fv and improvement of its binding affinity without loss of specificity. J Biol Chem 2002;277:2059–2064.
51. Lavoie TB, Mohan S, Lipschultz CA, Grivel J-C, Li Y, Mainhart CR, Kam-Morgan LNW, Drohan WN, Smith-Gill SJ. Structural differences among monoclonal antibodies with distinct fine specificities and kinetic properties. Mol Immunol 1999;36:1189–1205.
52. Brorson K, Thompson C, Wei G, Krasnokutsky M, Stein KE. Mutational analysis of avidity and fine specificity of anti-levan antibodies. J Immunol 1999;163:6694–6701.